ORIGINAL ARTICLE

Iterative Learning Control for Trajectory Tracking of Robot Manipulators

Tesheng Hsiao[1,*] and Po-Hao Huang[1]

[1]*Institute of Electrical and Control Engineering, National Chiao Tung University, Taiwan*

(**Received** 9 May 2017; **Accepted** 14 July 2017; **Published on line** 1 September 2017)

*Corresponding author: tshsiao@cn.nctu.edu.tw

DOI: 10.5875/ausmt.v7i3.1410

Abstract: Iterative learning control (ILC) has been shown to be effective in improving tracking performance of repetitive tasks, and is widely used in the motion control systems of CNC machines, semiconductor manufacturing equipment, hard disk drives, etc. However, applying ILC to robot manipulators requires careful consideration of nonlinear dynamics. We propose using a computed torque controller and the disturbance observer (DOB) to robustly linearize the dynamics of robot manipulators. The PD feedback controller is then applied for each joint to achieve the desired bandwidth and damping ratio. Both control-based ILC and command-based ILC are implemented separately in the linearized system as a feedforward compensator to enhance trajectory tracking accuracy. The proposed control system is realized in a six-axis industrial robot. Experimental results show that DOB is indispensable for robust feedback linearization so that ILC can work on the linearized system to improve the tracking performance for repetitive motion. Satisfactory and similar performance is accomplished by both control-based ILC and command-based ILC.

Keywords: computed torque, disturbance observer, iterative learning control, robot Manipulator, trajectory tracking

Introduction

Robot manipulators are widely used in production lines in tasks including assembling, welding, painting, deburring, polishing, etc. Increasing product complexity and miniaturization requires increased manufacturing precision and speed, raising significant challenges to robot motion control systems. Such control systems have been extensively investigated over the past few decades [1]. Among proposed control methodologies, iterative learning control (ILC) has attracted considerable attention recently because of its effectiveness in enhancing tracking performance of repetitive motions [2].

Conventional ILC is designed to control linear time-invariant systems in a feedforward manner by modifying either the control input or the command [3]. However, robot manipulators are known for their complicated nonlinearities, which must be carefully processed before ILC can be applied. Typical methods to deal with nonlinearities include linearization of the model along the trajectory, linearization by feedback control laws, and diminishing the nonlinear effects through the delicate design of electrical/mechanical systems.

The authors in [4,5] linearized the robot dynamics along the trajectory. Since the linearized system was just an approximation of the nonlinear one around the operating point, only local convergence of errors can be guaranteed, and the control performance was limited due to the approximation error. On the other hand, Norrlöf [4] and Zhao *et al.* [5] implemented their ILCs on commercial industrial robots with integrated feedback controllers. Due to the well-designed feedback controllers, the closed-loop dynamics of the robot manipulator was close to a linear system. ILC was then used for disturbance rejection by iteratively learning external disturbances [4], or for improving the absolute accuracy of the point-to-point movement by learning the kinematic parameters of the robot manipulator [5]. Although the commercial feedback controllers work well

for linearization, they are closed systems, meaning that end users are neither allowed to retrieve detailed information (e.g. motor currents), nor to modify key parameters of the robot (e.g. D-H parameters). Thus if an additional outer-loop controller or feedforward controller is added on top of the commercial feedback controllers, the available information and tunable parameters are very limited.

Nonlinear robot dynamics are dominated by linear joint motors whenever high gear-ratios are used [6]. Under these circumstances, a frequency-domain ILC was proposed for the robot manipulators [7]. In [8], the proposed robot manipulator was designed such that the 1st joint is much heavier than the other joints; therefore the dynamics of the 1st joint can be regarded as linear by neglecting the coupling effects of the other joints. The iterative learning input shaping technique was proposed to suppress the residual vibration of the 1st joint. However, ignoring nonlinearities like [7] and [8] can work only for a special class of robot manipulators. In addition, more applications of ILC to robot manipulators such as impedance control [9] and hybrid force/velocity control [10] have been reported.

Previous studies suggest that optimal performance requires combining the feedback linearization controller and feedforward ILC. However, despite the widespread use of ILC in robot motion control, few attempts have been made to create such an integrated design. Therefore, we propose a joint space trajectory tracking control system consisting of a *computed torque controller* to linearize the robot dynamics, a *disturbance observer* (DOB) to enhance robustness of the linearized system, a *proportional-derivative (PD) feedback controller* to achieve the desired bandwidth and damping ratio for each joint, and an *ILC* to further enhance tracking performance for repetitive tasks. Both control-based ILC and command-based ILC are considered. A unified control framework is developed to implement either ILC with the aforementioned computed torque, DOB, and PD controllers. The proposed control system is implemented on a six-axis industrial robot. Experimental results show robust and satisfactory performance.

This paper is organized as follows. Section II illustrates the dynamic model of the robot manipulator. Section III presents the proposed control system. Experimental verification is conducted in Section IV and Section V concludes the paper.

Tesheng Hsiao received his B.S. and M.S. degrees in control engineering from National Chiao Tung University, Taiwan, in 1995 and 1997 respectively, and the Ph.D. degree in mechanical engineering from the University of California, Berkeley, in 2005. He is currently an associate professor with the Department of Electrical and Computer Engineering at National Chiao Tung University, Taiwan. His research interests include advanced vehicle control systems, robot motion and compliance control, and CNC precision motion control.

Po-Hao Huang received his B.S. degree in Yuan-Ze University in Taiwan and purses his M.S. degree in the Institute of Electrical and Control Engineering, National Chiao Tung University, Taiwan. His research topics include robotics, motion control, and iterative learning control.

Dynamic Model of the Robot Manipulator

The dynamic equation of an *n*-joint robot manipulator is given as follows:

$$\mathbf{M}(\mathbf{q})\ddot{\mathbf{q}} + \mathbf{C}(\mathbf{q},\dot{\mathbf{q}})\dot{\mathbf{q}} + \mathbf{G}(\mathbf{q}) + \mathbf{F}(\dot{\mathbf{q}}) = \boldsymbol{\tau} + \boldsymbol{\tau}_d \quad (1)$$

where $\mathbf{q},\dot{\mathbf{q}},\ddot{\mathbf{q}} \in \mathbb{R}^n$ are respectively the joint position, velocity, and acceleration vectors. $\mathbf{M}(\mathbf{q}), \mathbf{C}(\mathbf{q},\dot{\mathbf{q}}) \in \mathbb{R}^{n\times n}$ respectively denote the inertia matrix, and Coriolis and centrifugal matrix. $\mathbf{G}(\mathbf{q}), \mathbf{F}(\dot{\mathbf{q}}) \in \mathbb{R}^n$ respectively are the gravitational and frictional torque vectors. $\boldsymbol{\tau}, \boldsymbol{\tau}_d \in \mathbb{R}^n$ respectively are the joint torque and external disturbance. Note that $\boldsymbol{\tau}_d$ could be non-repetitive. Suppose that

$$\begin{aligned}\mathbf{M}(\mathbf{q}) &= \mathbf{M}_0(\mathbf{q}) + \Delta\mathbf{M}(\mathbf{q})\\ \mathbf{C}(\mathbf{q},\dot{\mathbf{q}}) &= \mathbf{C}_0(\mathbf{q},\dot{\mathbf{q}}) + \Delta\mathbf{C}(\mathbf{q},\dot{\mathbf{q}})\\ \mathbf{G}(\mathbf{q}) &= \mathbf{G}_0(\mathbf{q}) + \Delta\mathbf{G}(\mathbf{q})\\ \mathbf{F}(\dot{\mathbf{q}}) &= \mathbf{F}_0(\dot{\mathbf{q}}) + \Delta\mathbf{F}(\dot{\mathbf{q}})\end{aligned}$$

where the subscript 0 denotes the nominal model and the symbols with Δ on the left denote model uncertainties.

We investigate the problem of robust tracking of a repeated trajectory in the joint space. In other words, the robot manipulator must repeatedly follow the same desired trajectory $\mathbf{q}_d(t) \in \mathbb{R}^n,\ 0 \le t \le T$, in the joint space. Under the influence of model uncertainties and external disturbance $\boldsymbol{\tau}_d$, we derive the joint torque $\boldsymbol{\tau}^j$ for the j^{th} trial, $j = 1,2,\cdots$, such that the joint angle of the j^{th} trial, $\mathbf{q}^j(t)$, gradually approaches $\mathbf{q}_d(t),\ 0 \le t \le T$, as *j* increases.

Proposed Control Law

Let the tracking error be $\tilde{\mathbf{q}} = \mathbf{q}_d - \mathbf{q}$. Then the unified framework of the proposed control law is

$$\begin{aligned}\boldsymbol{\tau} = \mathbf{M}_0(\mathbf{q})\left(\ddot{\mathbf{q}}_d + \mathbf{u}_{fb} + \mathbf{u}_{DOB} - \mathbf{u}_{ILC}\right)\\ +\mathbf{C}_0(\mathbf{q},\dot{\mathbf{q}})\dot{\mathbf{q}} + \mathbf{G}_0(\mathbf{q}) + \mathbf{F}_0(\dot{\mathbf{q}}_d)\end{aligned} \quad (2)$$

where $\mathbf{u}_{fb}, \mathbf{u}_{DOB}, \mathbf{u}_{ILC}$ respectively denote the control inputs from the feedback controller, DOB and control-based ILC. These control inputs will be introduced shortly. We can see that (2) is in the form of the computed torque controller that cancels the nominal nonlinearities of (1). Note that $\dot{\mathbf{q}}_d$ is used instead of $\dot{\mathbf{q}}$ in the friction term of (2) to avoid chattering caused by the measurement noise in $\dot{\mathbf{q}}$ and the switching term in $\mathbf{F}_0$ that represents the Coulomb friction.

Substitute (2) into (1) and note that $\mathbf{M}_0(\mathbf{q})$ is

positive definite for all values of $\mathbf{q}$. Then we have

$$\ddot{\tilde{\mathbf{q}}} = -\mathbf{u}_{fb} - \mathbf{u}_{DOB} + \mathbf{u}_{ILC} + \mathbf{d} \quad (3)$$

where $\mathbf{d} = \mathbf{M}_0^{-1}(\mathbf{q})(\mathbf{h} - \boldsymbol{\tau}_d)$ and

$\mathbf{h} = \Delta\mathbf{M}(\mathbf{q})\ddot{\mathbf{q}} + \Delta\mathbf{C}(\mathbf{q}, \dot{\mathbf{q}})\dot{\mathbf{q}} + \Delta\mathbf{G}(\mathbf{q}) + \mathbf{F}(\dot{\mathbf{q}}) - \mathbf{F}_0(\dot{\mathbf{q}}_d)$ is the uncertain term.

PD Feedback Controller

Let the PD feedback controller be used here, i.e.

$$\mathbf{u}_{fb} = -\left[\mathbf{K}_d\left(\dot{\mathbf{r}} - \dot{\tilde{\mathbf{q}}}\right) + \mathbf{K}_p(\mathbf{r} - \tilde{\mathbf{q}})\right] \quad (4)$$

where $\mathbf{K}_p, \mathbf{K}_d \in \mathbb{R}^{n\times n}$ are positive definite diagonal matrices, i.e. $\mathbf{K}_p = \text{diag}(k_{p1}, \cdots k_{pn})$ and $\mathbf{K}_d = \text{diag}(k_{d1} \cdots k_{dn})$, where diag$(\cdot)$ denotes a diagonal matrix and $k_{pi}, k_{di} > 0$ for $i = 1, \cdots, n$. $\mathbf{r}$ is the control input from the command-based ILC, which will be introduced later. Then for each joint, (3) and (4) can be expressed as the block diagram in Figure 1, where the subscript *i* denotes the *i*th joint, $i = 1, \cdots, n$. By properly setting the PD gains k_{pi} and k_{di}, we can achieve the desired damping ratio and bandwidth for the *i*th joint.

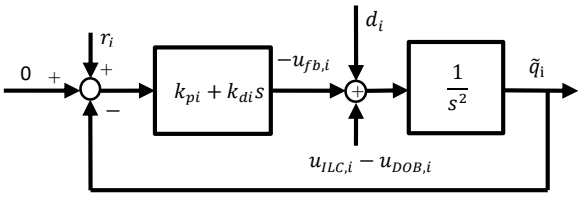

Figure 1. Block diagram of the *i*th joint based on (3) and (4).

Disturbance Observer

The disturbance $\mathbf{d}$ degenerates the desired performance set by the PD controller; DOB is introduced to overcome this problem. We redraw the system from $-u_{fb,i}$ to $\tilde{q}_i$ in Figure 1 and include DOB explicitly as shown in Figure 2, where $Q_{DOB,i}(s)$ is a low-pass filter with a relative degree greater than 2. Then from Figure 2 we have

$$u_{DOB,i}(s) = \frac{Q_{DOB,i}(s)s^2}{1-Q_{DOB,i(s)}}\tilde{q}_i(s) - \frac{Q_{DOB,i}(s)}{1-Q_{DOB,i(s)}}u_i(s) \quad (5)$$

where $u_i = u_{ILC,i} - u_{fb,i}$.

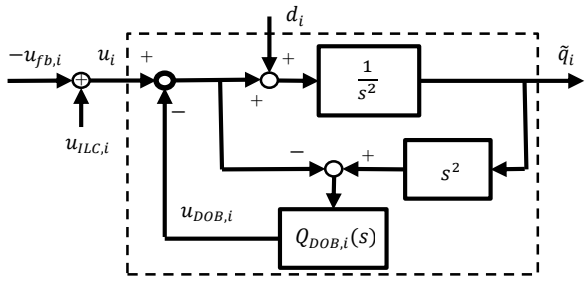

Figure 2. Robot motion controller with DOB.

Remark: We do not implement the double differentiators in Figure 2; instead, (5) is used to realize DOB. Note that both $\frac{Q_{DOB,i}(s)s^2}{1-Q_{DOB,i(s)}}$ and $\frac{Q_{DOB,i}(s)}{1-Q_{DOB,i(s)}}$ are proper.

Furthermore,

$$\tilde{q}_i(s) = \frac{1}{s^2}u_i(s) + \frac{1}{s^2}\left(1 - Q_{DOB,i}(s)\right)d_i(s) \quad (6)$$

Hence, at the low frequency band where $Q_{DOB}(s) \approx 1$, d_i is eliminated and thus $\tilde{q}_i(s) \approx \frac{1}{s^2}u_i(s)$. On the other hand, at the high frequency band where $Q_{DOB}(s) \approx 0$, we have

$$\tilde{q}_i(s) = \frac{1}{s^2}\left(u_i(s) + d_i(s)\right)$$

as if DOB did not exist.

Combining (4) and (6) yields

$$\tilde{q}_i(s) = G_i(s)\left[u_{ILC,i}(s) + \left(k_{pi} + k_{di}s\right)r_i(s) + \left(1 - Q_{DOB,i}(s)\right)d_i(s)\right] \quad (7)$$

where $G_i(s) = \frac{1}{s^2 + k_{di}s + k_{pi}}$.

To further improve tracking performance, we apply either control-based ILC (from $\mathbf{u}_{ILC}$) or command-based ILC (from $\mathbf{r}$) to eliminate the repetitive component in $\mathbf{d}$ and in other unmodeled sources. The ILC design is discussed in the subsequent subsections.

Control-based ILC

In Figure 2, the control-based ILC $u_{ILC,i}$ modifies $u_{fb,i}$ based on the control input and the error of the previous trial. To determine $u_{ILC,i}$, we let r_i in (7) be zero and discretize (7) as follows:

$$\tilde{q}_i(k) = \bar{G}_i(z)u_{ILC,i}(k) + d_i'(k) \quad (8)$$

where $\bar{G}_i(z)$ is the discrete-time counterpart of $G_i(s)$ and $d_i' = G_i(s)\left(1 - Q_{DOB,i}(s)\right)d_i$. $\tilde{q}_i$ is regarded as the output of (8), and the objective of the control-based ILC is to regulate $\tilde{q}_i$ to zero. Therefore the control-based ILC is

$$u_{ILC,i}^{j+1}(k) = Q_{ti}(z)\left(u_{ILC,i}^{j}(k) + L_{ti}(z)\tilde{q}_i^{\,j}(k+1)\right)$$

where the superscript *j* denotes the *j*th trial. $L_{ti}(z) = \bar{G}_i^{-1}(z)$ is the learning filter. $Q_{ti}(z)$ is the robust filter, which is a low-pass filter with a relative degree larger than one. The block diagram consisting of the feedback controller and the control-based ILC is shown in Figure 3.

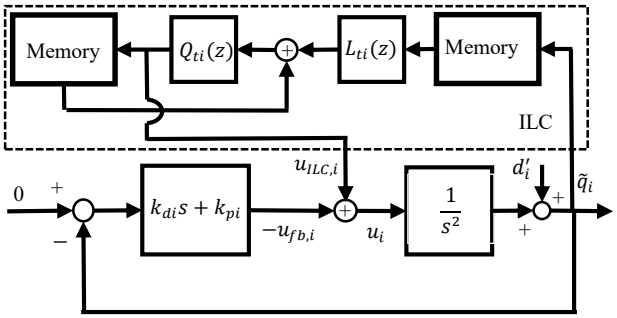

Figure 3. Control-based ILC.

From the theorem of ILC, $\tilde{q}_i^{\,j}$ converges to

$$\tilde{q}_i^{\infty}(z) = \frac{1 - Q_{ti}(z)}{1 - Q_{ti}(z)\left(1 - zL_{ti}(z)\bar{G}_i(z)\right)}d_i'(z)$$

as $j \to \infty$ if the following condition holds [3]

$$\|Q_{ti}(z)(1 - zL_{ti}(z)\bar{G}_i(z))\|_\infty < 1$$

Remarks:

1. $G_i(s)$ is composed of the feedback loop of a double integrator and a PD controller (see Figure 1); therefore $G_i(s)$ is known exactly without model uncertainty. However the robust filter is still required since the disturbance d_i' may contain non-repetitive components which are not cancelled by the disturbance observer.
2. The properties of minimum phase and relative degree may not be preserved during the conversion from $G_i(s)$ to $\bar{G}_i(z)$; however, it can be shown that if $G_i(s)$ is critically damped and the conversion is based on the impulse invariance method, then $\bar{G}_i(z)$ is a minimum phase system with a relative degree of one. The proof is presented in the Appendix.
3. Many design methods for the learning filter and the robust filter of ILC have been proposed [3]. Since there are no model uncertainties and no non-minimum phase zeros in $\bar{G}_i(z)$, the plant inversion method is used here to achieve the fastest convergence rate. The experimental results presented in the next section show that the ILC converges in just one iteration (see Figure 7). The only problem of the plant inversion method is the non-causality of the learning filter. However, it can be solved by choosing the robust filter with a sufficiently large relative degree.

Command-based ILC

Now, we consider the command-based ILC. Suppose that $u_{ILC,i} = 0$; then (7) becomes

$$\tilde{q}_i(s) = G_{ri}(s)r_i(s) + d_i' \tag{9}$$

where $G_{ri}(s) = \frac{k_{di}s + k_{pi}}{s^2 + k_{di}s + k_{pi}}$.

Let $\bar{G}_{ri}(z)$ be the discrete-time counterpart of $G_{ri}(s)$. Then the command-based ILC is

$$r_i^{j+1}(k) = Q_{ri}(z)\left(r_i^j(k) + L_{ri}(z)\tilde{q}_i^j(k+1)\right)$$

where the learning filter is $L_{ri}(z) = \bar{G}_{ri}^{-1}(z)$. The robust filter $Q_{ri}(z)$ is a low-pass filter with a relative degree greater than two. The block diagram consisting of the feedback controller and the command-based ILC is shown in Figure 4. Similar to the control-based ILC, $\tilde{q}_i^j$ converges to

$$\tilde{q}_i^\infty(z) = \frac{1 - Q_{ri}(z)}{1 - Q_{ri}(z)\left(1 - zL_{ri}(z)\bar{G}_{ri}(z)\right)} d_i'(z)$$

as $j \to \infty$ if the following condition holds

$$\|Q_{ri}(z)(1 - zL_{ri}(z)\bar{G}_{ri}(z))\|_\infty < 1$$

Remark: The Appendix shows that if $G_{ri}(s)$ is critically damped and the conversion to $\bar{G}_{ri}(z)$ is based on the impulse invariance method, then $\bar{G}_{ri}(z)$ is a minimum phase system with a relative degree of zero.

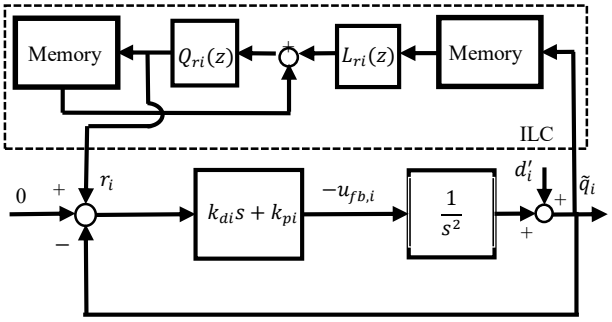

Figure 4. Command-based ILC.

Experimental Results

The proposed control law is implemented on a personal computer (PC) to control a RA605 6-axis industrial robot made by Hiwin Technologies Corp, Taiwan (Figure 5). The drivers of joint motors are placed in an electrical cabinet and the PC-based controller sends torque commands to the drivers through an EtherCAT network. A 17-bit absolute encoder is installed in each joint motor to measure the joint angle, and the joint velocity is obtained by numerical differentiation of the joint position. The gear ratios for joints 1~6 are respectively 80, 100, 80, 81, 80, 50.

The sampling time is 1ms, and the gains of the PD controller are chosen as

$$\mathbf{K}_p = \text{diag}(3600,1600,1225,2500,5625,11025)$$
$$\mathbf{K}_d = \text{diag}(120,80,70,100,150,210)$$

Figure 5. RA605 6-axis Industrial Robot.

With these gains, the linearized joint dynamics are critically damped for all joints, and the (undamped) natural frequencies for joints 1~6 are respectively 60, 40, 35, 50, 75, 105 (rad/sec) for joint 1~6. In designing $Q_{DOB,i}(s)$, a low order filter is preferred because it avoids introducing excessive phase lag into the closed-loop system. The cutoff frequency is tuned by trial and error to minimize disturbance without jeopardizing system stability. Therefore $Q_{DOB,i}(s)$ is designed as a

second-order Butterworth low-pass filter with cutoff frequencies at 15, 15, 8, 15, 30, 30 (Hz) corresponding to $i = 1, \cdots, 6$. For both the control-based ILC and command-based ILC, the robust filters $Q_{ti}(z)$ and $Q_{ri}(z)$ have cutoff frequencies at 20, 13, 20, 10, 13, 13 (Hz) respectively for joints 1~6.

The test trajectory in the joint space is shown in Figure 6. For each joint, the trajectory is a mixture of sinusoidal signals with 4 different frequencies up to 3 Hz. Therefore this trajectory represents an arbitrary fast movement of the robot in a small range, and it is designed to test the tracking accuracy and bandwidth of the proposed controller.

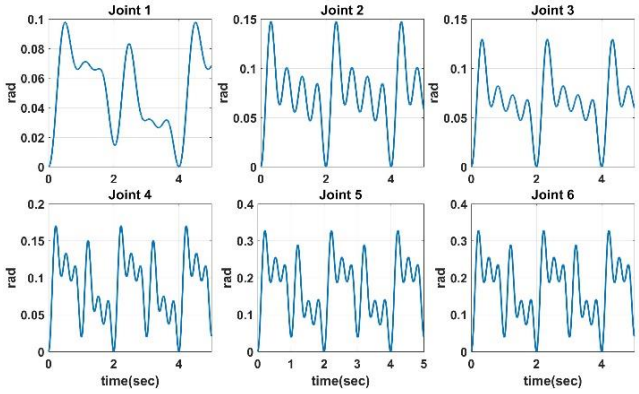

Figure 6. The test trajectory in the joint space.

Experiments on tracking the test trajectory were conducted repetitively to verify the performance of both control-based and command-based ILC. Figure 7 shows the root-mean-square (RMS) tracking error of each joint as the number of iteration increases. From Figure 7, we can see that both ILCs converge at the first iteration and are stable as the number of iterations increases. This fast convergence can be attributed to the use of plant inversion as the learning filters in both ILCs.

As shown in the previous section, the proposed control law contains several components including computed torque controller, PD feedback controller, DOB, and control-based ILC or command-based ILC. To verify the contribution of each component, we repeat the experiments with four control systems that include different combinations of the aforementioned components. These control systems are (1) computed torque plus PD feedback controller (CT), (2) computed-torque plus PD feedback controller and DOB (CT+DOB), (3) computed torque plus PD feedback controller, DOB, and control-based ILC (CT+DOB+Ctrl-ILC), and (4) computed torque plus PD feedback controller, DOB, and command-based ILC (CT+DOB+Cmd-ILC). According to Figure 7, we choose the data in the 5th iteration of both types of ILCs for comparison with other control systems.

Experimental results are shown in Figure 8. The maximum and RMS errors of each joint are summarized in Table 1. It can be seen that the computed torque plus PD feedback controller has the largest errors in all joints because of the uncompensated model uncertainties. Introducing DOB in the control loop significantly improves the tracking accuracy because a large portion of the model uncertainties are eliminated by DOB. Two types of ILCs are included as feedforward compensators to further reduce the tracking error. Generally speaking, ILC improves the tracking performance by compensating for external disturbances, model uncertainties, and the servo lag. However, in the proposed control system, the plant models for both ILCs (i.e. $\bar{G}_i(z)$ and $\bar{G}_{ri}(z)$) have no uncertainties, while the "equivalent commands" to both ILCs are zeros (see Figure 3 and Figure 4), making the "servo lag" irrelevant to the tracking performance. The performance enhancement by ILC mainly comes from rejecting the disturbance d_i'. In the experiments, however, the repetitive portion of the disturbance resulting from the repeated trajectory has a low bandwidth (up to 3 Hz); therefore most parts of the

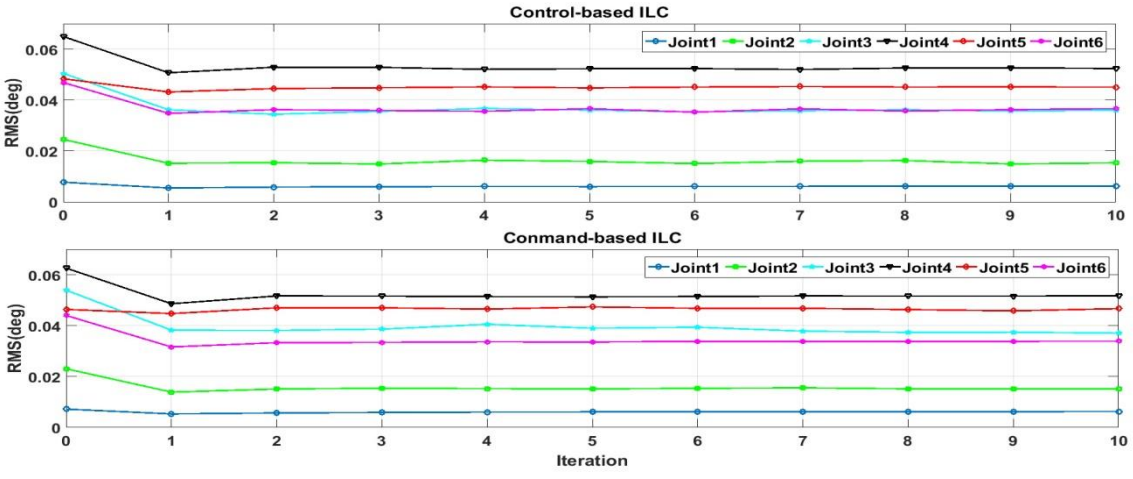

Figure 7. RMS error for each iteration.

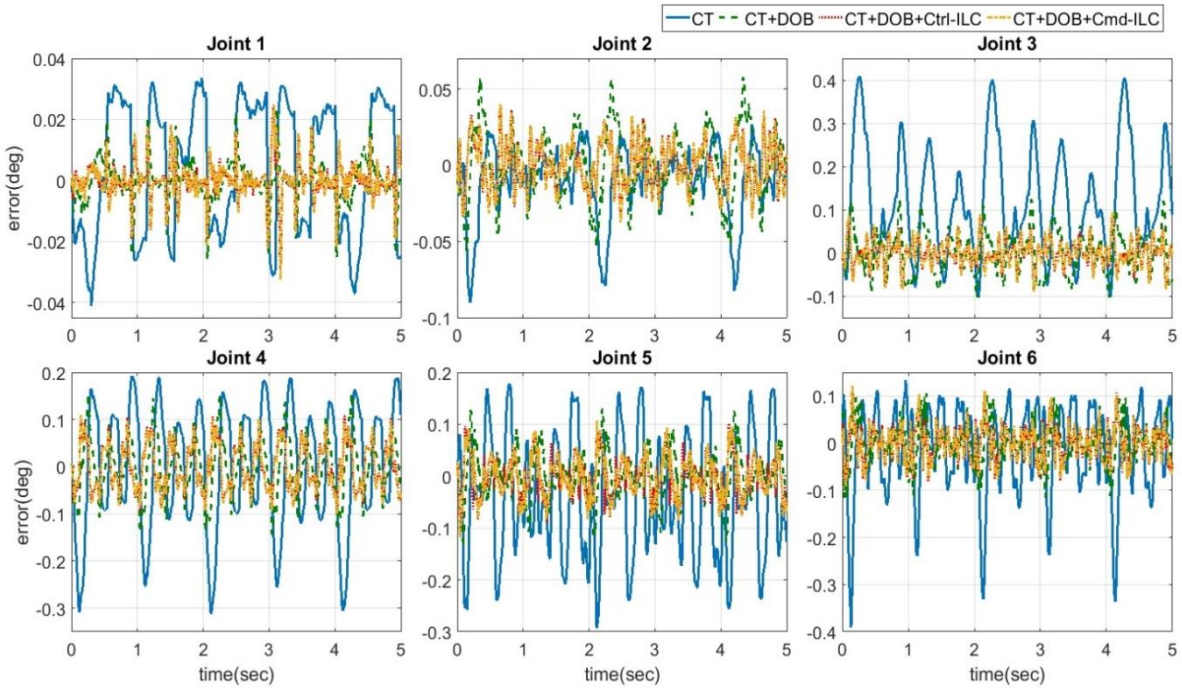

Figure 8. Experimental Results.

repetitive disturbance are cancelled by DOB leaving little for ILC. Consequently, both types of ILCs only produce slight reductions to the tracking errors. The control-based ILC has the smallest tracking errors in almost all joints, but both ILCs have similar performance.

The results show that the computed torque controller is effectively in principle for linearizing and decoupling a complicated nonlinear system such as the robot manipulator, and that the linearized system can achieve the desired damping ratio and natural frequency by using a simple PD feedback controller. However, the computed torque controller is very sensitive to model uncertainties, leading to poor performance in practice.

The experiments show that DOB is indispensable for rejecting disturbance and model uncertainties. By introducing DOB in the control loop, the robot manipulator can be robustly linearized and then both control-based ILC and command-based ILC can be applied. Experimental data show that ILC improves the tracking performance for repetitive motion, and both types of ILC have similar performance.

Remark: Although ILC can reduce model uncertainties, it is effective only for repetitive motions. The ultimate goal of the proposed robot control system is to achieve high tracking performance for most tasks, including repetitive and non-repetitive ones. Therefore, using DOB for robust linearization is preferable due to its wide applicability. As a result, the proposed control scheme can turn off ILC to accomplish highly accurate non-repetitive tasks, and turn on either control-based ILC or command-based ILC to further reduce tracking errors for repetitive tasks. Since the combinations of CT+Ctrl-ILC and CT+Cmd-ILC restrict the applications of the control system to only repetitive tasks, they are not included in the experiments for comparison.

Table 1. Summary of the control performance for different controllers.

Joint		1	2	3	4	5	6
CT	MAX (deg)	0.041	0.090	0.409	0.312	0.293	0.391
	RMS (deg)	0.022	0.025	0.174	0.131	0.124	0.098
CT+DOB	MAX (deg)	0.026	0.058	0.123	0.156	0.137	0.115
	RMS (deg)	0.008	0.023	0.051	0.063	0.047	0.045
CT+DOB+Ctrl-ILC	MAX (deg)	0.031	0.039	0.092	0.107	0.114	0.111
	RMS (deg)	0.006	0.015	0.030	0.050	0.039	0.036
CT+DOB+Cmd-ILC	MAX (deg)	0.033	0.040	0.092	0.109	0.118	0.123
	RMS (deg)	0.007	0.015	0.032	0.049	0.040	0.036

Conclusion

We applied ILC for trajectory tracking of robot manipulators in the joint space. The computed torque controller and DOB are used first to robustly linearize the highly nonlinear dynamics of robot manipulators. Then ILC is applied to the linearized system. Both control-based ILC and command-based ILC are implemented. Experimental results show that both types of ILC improve tracking accuracy and achieve similar performance.

Appendix

This appendix shows that $\bar{G}_i(z)$ and $\bar{G}_{ri}(z)$ in Section III are minimum phase systems with respective relative degrees of one and zero.

Lemma: Let $G_i(s) = \frac{1}{s^2+k_{di}s+k_{pi}}$ and $G_{ri}(s) = \frac{k_{di}s+k_{pi}}{s^2+k_{di}s+k_{pi}}$, where $k_{di}, k_{pi} > 0$. Suppose that $\bar{G}_i(z)$ and $\bar{G}_{ri}(z)$ are respectively the discrete-time counterparts of $G_i(s)$ and $G_{ri}(s)$ which are obtained by the impulse invariance method. If $G_i(s)$ and $G_{ri}(s)$ are critically damped, then $\bar{G}_i(z)$ and $\bar{G}_{ri}(z)$ are minimum phase systems with respective relative degrees of one and zero.

Proof: Since $G_i(s)$ and $G_{ri}(s)$ are critically damped, they have multiple poles at $r = -\sqrt{k_{pi}} < 0$. Therefore $G_i(s)$ and $G_{ri}(s)$ can be decomposed as follows:

$$G_i(s) = \frac{1}{(s-r)^2}, \qquad G_{ri}(s) = \frac{A_1}{s-r} + \frac{A_2}{(s-r)^2}$$

where $A_1 = k_{di} = 2\sqrt{k_{pi}}$ and $A_2 = -k_{pi}$.

Discretizing $G_i(s)$ and $G_{ri}(s)$ by the impulse invariance method yields

$$\bar{G}_i(z) = \frac{T^2 e^{rT} z^{-1}}{(1-e^{rT}z^{-1})^2} = \frac{T^2 e^{rT} z}{(z-e^{rT})^2}$$

$$\bar{G}_{ri}(z) = \frac{TA_1 + Te^{rT}(TA_2 - A_1)z^{-1}}{(1-e^{rT}z^{-1})^2} = \frac{TA_1 z^2 + Te^{rT}(TA_2 - A_1)z}{(z-e^{rT})^2}$$

Clearly, the relative degree of $\bar{G}_i(z)$ is one, and the only finite zero is at $z = 0$. Hence $\bar{G}_i(z)$ is minimum phase.

On the other hand, the relative degree of $\bar{G}_{ri}(z)$ is zero, and the two finite zeros locate at $z = 0$ and

$$z = -\frac{e^{rT}(TA_2 - A_1)}{A_1} = e^{-\sqrt{k_p}T}\left(\frac{\sqrt{k_p}T}{2} + 1\right) \qquad (10)$$

Obviously, (10) is always positive. Moreover, if we treat the right hand side of (10) as a function of $\sqrt{k_p}T$, then it can be shown that $z(\sqrt{k_p}T)$ is a strictly decreasing function. Therefore

$$0 < z\left(\sqrt{k_p}T\right) < z(0) = 1, \qquad \forall k_p > 0$$

This validates that $\bar{G}_{ri}(z)$ is a minimum phase system.

References

[1] T. Hsiao and M.-C. Weng, "Robust Joint Position Feedback Control of Robot Manipulators," *ASME Journal of Dynamic Systems, Measurement, and Control,* vol. 135, no. 3, pp. 031010-1-031010-11, March 2013. doi: 10.1115/1.4023669

[2] R. W. Longman, "Iterative Learning Control and Repetitive Control for Engineering Practice," *International Journal of Control,* vol. 73, no. 10, pp. 930-954, July 2000. doi: 10.1080/002071700405905

[3] D. A. Bristow, M. Tharayil, and A. G. Alleyne, "A Survey of Iterative Learning Control," *IEEE Control Systems,* vol. 36, no. 3, pp. 96-114, May 2006. doi: 10.1109/MCS.2006.1636313

[4] M. Norrlöf, "An Adaptive Iterative Learning Control Algorithm with Experiments on an Industrial Robot," *IEEE Transactions on Robotics and Automation,* vol. 18, no. 2, pp. 245-251, Apr. 2002. doi: 10.1109/TRA.2002.999653

[5] Y.-M. Zhao, Y. Lin, F. Xi, and S. Guo, "Calibration-Based Iterative Learning Control for Path Tracking of Industrial Robots," *IEEE Transactions On Industrial Electronics,* vol. 62, no. 5, pp. 2921-2929, Oct. 2015. doi: 10.1109/TIE.2014.2364800

[6] R. Kelly, V. S. Davila, and A. Loria, *Control of Robot Manipulators in Joint Space*. London, UK: Springer London, 2005.

[7] A. De Luca, G. Paesano, and G. Ulivi, "A Frequency-Domain Approach to Learning Control: Implementation for a Robot Manipulator," *IEEE Transactions on Industrial Electronics,* vol. 39, no. 1, pp. 1-10, Feb. 1992. doi: 10.1109/41.121905

[8] J. Park, P.-H. Chang, H.-S. Park, and E. Lee, "Design of Learning Input Shaping Technique for Residual Vibration Suppression in an Industrial Robot," *IEEE/ASME Transactions on Mechatronics,* vol. 11, no. 1, pp. 55-65, Feb. 2006. doi: 10.1109/TMECH.2005.863365

[9] C.-C. Cheah and D. Wang, "Learning Impedance Control for Robotic Manipulators," *IEEE Transactions on Robotics and Automation,* vol. 14, no. 3, pp. 452-465, Jun. 1998. doi:10.1109/70.678454

[10] A. Visioli, G. Ziliani, and G. Legnani, "Iterative-Learning Hybrid Force/Velocity Control for Contour Tracking," *IEEE Transactions on Robotics,* vol. 26, no. 2, pp. 388-393, Feb. 2010. doi: 10.1109/TRO.2010.2041265